Probing the colloidal gold nanoparticle/aqueous interface with second harmonic generation

Louis H. Haber, Sheldon J.J. Kwok, Monica Semeraro [1], Kenneth B. Eisenthal *

Department of Chemistry, Columbia University, New York, NY 10027, USA

ARTICLE INFO

ABSTRACT

The interface of 16 nm colloidal gold nanoparticles with the aqueous solution in which they are suspended is investigated using second harmonic generation. The population of malachite green freely adsorbing to the gold nanoparticle interface as a function of concentration is obtained. The experimental results are in good agreement with the modified Langmuir model, which includes depletion of the adsorbate bulk concentration. The free energy of adsorption is determined to be -15.4 ± 0.4 kcal/mol with $1.13 \pm 0.04 \times 10^3$ sites per nanoparticle. These results provide the first direct measurement of the isotherm of molecules adsorbing to colloidal metallic nanoparticles.

© 2011 Published by Elsevier B.V.

1. Introduction

The study of the interface of metallic nanoparticles with the liquid in which they are suspended is motivated by their unique optical, electronic, and chemical properties. These special characteristics are a consequence of their ultra small dimensions, compositions, and shapes, which influence the localized surface plasmon resonances that involve the coherent oscillations of conduction electrons [1,2]. The size and shape of metallic nanoparticles can be controlled to nanometer scales using different solution-based methods of synthesis [1,2]. The capping agent required to stabilize the particles in solution can be changed to alter the nanoparticle functionality [2,3]. The surface plasmons can couple with the incident light and greatly enhance optical signals such as surface enhanced Raman scattering (SERS) [4,5] and surface enhanced fluorescence [6,7], as well as enhanced nonlinear optical processes such as sum-frequency generation (SFG) [8,9] and second harmonic generation (SHG) [10–13]. Gold nanoparticles, in particular because they are biologically inert, are well suited for many biologically-relevant technologies such as sensing [14,15], labeling [16], and photothermal cancer therapy [17]. However, to maximize the applicability of noble metal nanoparticles to science and technology, more research is required to better understand chemical and physical interactions at the nanoparticle surface.

A powerful technique for investigating the chemical and physical properties of molecules at colloidal nanoparticle surfaces utilizes second harmonic generation [18] and sum frequency generation [19–22]. The key attribute of these second order spectroscopies is that they are interface selective for reasons of symmetry [23–26]. The application of SHG to the study of interfacial phenomena complements important work in which molecules of interest are covalently bound to the surface of metal nanoparticles [2,6,7,27,28]. Previous SHG studies on the free adsorption of the triphenyl methane dye, malachite green (MG), to the surface of colloidal polystyrene microparticles has allowed the free energy of adsorption as well as the maximum number of adsorbate sites to be determined [29,30]. This SHG research has since been extended to study the adsorption of molecules to a variety of types and sizes of colloidal polymer microparticles and nanoparticles [31–35], clay [36], TiO$_2$ [37], and carbon black [38] nanoparticles, oil droplets in water [30], as well as phospholipid liposomes bilayer membranes [39,40]. Related work using SHG to measure the surface electrostatic potential [41] and the surface acidity pK_a [42] of nanoparticles has also been achieved.

In this Letter, we report the use of SHG to monitor the adsorption isotherm of malachite green to the surface of an ensemble of 16 nm colloidal gold nanoparticles in water. Malachite green is selected because it is cationic and has a large hyperpolarizability at our laser wavelength, giving a large SHG signal when it binds to the negatively-charged gold surface. The measured adsorption isotherm is in good agreement with the modified Langmuir model that includes depletion of the bulk adsorbate concentration. The experimental results provide for the free energy of adsorption as well as the adsorbate site density.

2. Experimental

2.1. Nanoparticle synthesis and characterization

The colloidal gold nanoparticle sample is synthesized from the reduction of chloroauric acid by citrate using the standard

Turkevich method [1,2,43]. All chemicals are purchased from Sigma–Aldrich and used without further purification in nanopure water. A 160 mL solution of 260 μM $HAuCl_4$ is brought to a light boil under vigorous stirring followed by the addition of 3.2 mL of 34 mM $Na_3C_6H_5O_7$. The solution changes color from a pale yellow to a bright red over approximately 15 min, and the boiling is continued for an additional 30 min. After cooling to room temperature, 10 mL of the nanoparticle solution is dialyzed against 150 mL of 20 μM trisodium citrate for two days. Dialysis is done to reduce the salt concentration to a known quantity and to prevent the nanoparticles from aggregating during the adsorption measurements, as confirmed by dynamic light scattering. The sample is diluted by adding 53 ml of water to 7 ml of the dialyzed sample and the pH is brought to 4.5 using hydrochloric acid to ensure that the malachite green adsorbate is in its cationic form.

The nanoparticle sample is characterized with transmission electron microscopy (TEM), linear absorption spectroscopy, and dynamic light scattering (DLS). Figure 1 shows a TEM image of the gold nanospheres on a carbon foil grid. A survey of over 200 nanoparticle TEM images determines the nanoparticle diameter to be 16.0 ± 1.5 nm. An absorption spectrum of the nanoparticle solution is displayed in Figure 2, showing the localized surface plasmon resonance peak to be centered at 520 nm. The absorption spectrum is compared to Mie Theory [1,44] at the measured size distribution showing good agreement for a concentration of $6.6 ± 0.1 \times 10^{10}$ nanoparticles/mL. The nanoparticle hydrodynamic diameter is measured to be 16.5 ± 1.7 nm using dynamic light scattering, which is in good agreement with the TEM results. The nanoparticle sample is observed to be stable over several months when kept under refrigeration at 4 °C.

2.2. Second harmonic generation

The second harmonic generation measurements of the adsorption isotherm of malachite green to the surface of colloidal gold nanoparticles are performed with an experimental setup that has been described previously [42], with a few important modifications. A titanium:sapphire oscillator is pumped by a 4.5 W
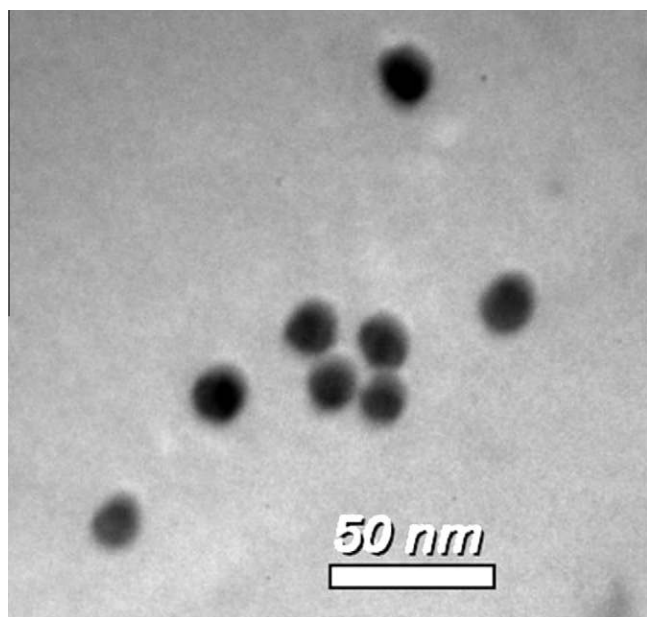
Figure 1. Transmission electron microscopy image of gold nanoparticles on a carbon foil grid. A survey of over 200 nanoparticle images shows the nanoparticle diameter to be 16.0 ± 1.5 nm.
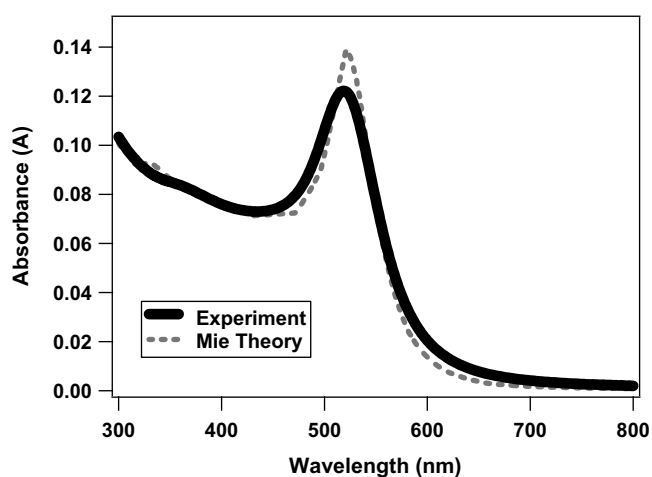

Figure 2. Absorption spectrum of the 16.0 ± 1.5 nm colloidal gold nanoparticles in water (black line) compared to the best fit using Mie Theory (dotted gray line). The absorption spectrum of the nanoparticle sample does not change after exposure to the laser.

532 nm Nd:YVO$_4$ laser producing 80 fs pulses centered at 816 nm with a repetition rate of 82 MHz and an average power of 500 mW. A 6.4 cm focal length lens focuses the p-polarized laser pulses to the colloidal sample in a 1 cm quartz cuvette at room temperature. The SHG light is collected at 90° and is refocused to a detector through a filter to remove scattered fundamental 816 nm light. The detector consists of a monochromator in front of a photon-counting photomultiplier tube (PMT) connected to a computer. A computer-controlled burette adds a high concentration malachite green solution to the colloidal nanoparticle sample during automated stirring. Several spectral scans are acquired for each addition of malachite green to ensure that a stable equilibrium is reached, and the isotherm is acquired several times for statistical analysis.

3. Results and discussion

The spectra are analyzed for each concentration of malachite green added to the nanoparticle sample and are used to obtain the adsorption isotherm. Figure 3 displays representative spectra showing two peaks. The shorter wavelength peak is attributed to second harmonic generation and the other peak to MG two-photon fluorescence. The SHG and fluorescence signals are seen to be very weak for the nanoparticle solution without MG. Double-Gaussian fits to the spectra show the two peaks to be centered at 407.9 ± 0.3 and 450 ± 2 nm, respectively, with full-width half maxima of 12.6 ± 0.7 and 73 ± 7 nm, respectively. The peaks centers and widths stay constant to within experimental uncertainty for all MG concentrations. The SHG peak at 408 nm corresponds to twice the laser frequency, as expected, and its signal is seen to rise as MG is added, reaching a maximum value as the MG adsorbed to the gold nanoparticle interface comes to its saturation value. The peak at 450 nm corresponds to two-photon fluorescence of the MG [45] which is enhanced by approximately 350% compared to a solution of MG without nanoparticles. The SHG signal obtained from the double-Gaussian fits of the spectra from each MG concentration is used to determine the adsorption isotherm.

The experimental isotherm of MG adsorbing to the gold nanoparticle surface, shown in Figure 4, is compared to the best fits to the Langmuir and the modified Langmuir models [30]. The SHG electric field E_{SHG} is proportional to the population of MG on the nanoparticle surface multiplied by the concentration of nanoparticles, N. In Figure 4, E_{SHG} is normalized to its maximum value found
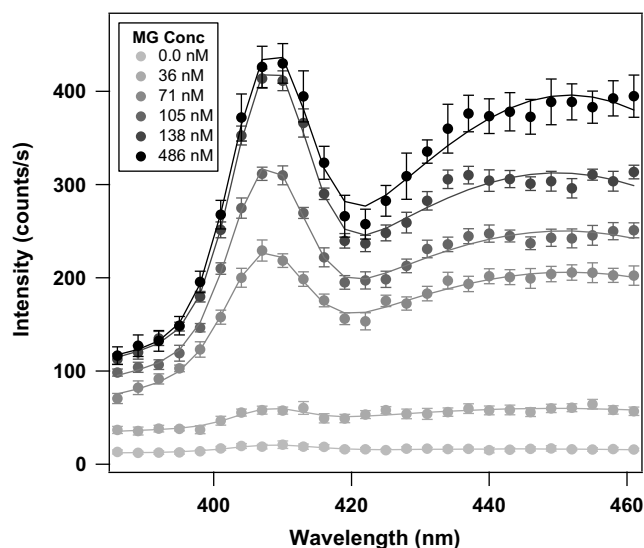
Figure 3. Spectra of the colloidal gold nanoparticles with varying malachite green concentrations showing second harmonic generation and two-photon fluorescence with double-Gaussian best fits.
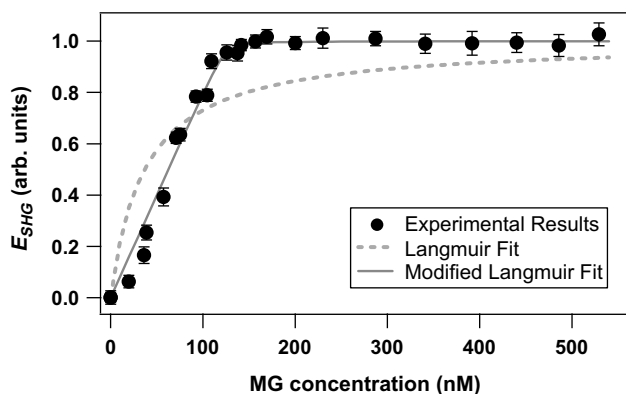
Figure 4. Experimental results (black circles) of the adsorption isotherm show the second harmonic electric field as a function of malachite green concentration. The density of the gold nanoparticles is $6.6 \pm 0.1 \times 10^{10}$ nanoparticles/mL. A comparison of the fits for the Langmuir (dotted gray line) and the modified Langmuir (solid gray line) is shown.

at the isotherm's plateau. E_{SHG} of the nanoparticle sample with no MG added is negligible compared to E_{SHG} at the isotherm's plateau, so possible phase-sensitive interferences [38] are neglected. In the Langmuir model, a key assumption is that the bulk concentration of the solute is not reduced by the solute adsorption to the interface. For a planar interface, this assumption is generally reasonable because the interface population is negligible compared to the solute population in the bulk solution. Unlike the planar interface, the nanoparticle density in the bulk solution, even at low densities, provides a cumulatively large surface area to which molecules can adsorb. Thus there can be a reduction in the bulk concentration of adsorbing molecules by the nanoparticles in the bulk solution. The modified Langmuir model includes this depletion of the adsorbate from the bulk solution, with the adsorbate population on the nanoparticle surface given by

$$\frac{N}{N_{max}} = \frac{(C + N_{max} + \frac{55.5}{K}) - \sqrt{(C + N_{max} + \frac{55.5}{K})^2 - 4CN_{max}}}{2N_{max}} \quad (1)$$

where C is the adsorbate bulk concentration added, N_{max} is the maximum number of adsorbate sites on the nanoparticle surface multiplied by the concentration of nanoparticles in the solution, and K is the adsorption equilibrium constant.[30] Eq. (1) reduces to the Langmuir model in the limit of $55.5/K \gg N_{max}$. The best fits of the Langmuir and modified Langmuir models to the experimental results of the adsorption isotherm provide information on the free energy of adsorption as well as the maximum number of adsorbate sites on each nanoparticle. The best fit for the Langmuir model gives an adsorption equilibrium constant of $K = 1.5 \pm 0.3 \times 10^9$ and a free energy of adsorption of $\Delta G° = -12.5 \pm 0.1$ kcal/mol, where $\Delta G° = -RT \ln K$. However, Figure 4 clearly shows that the Langmuir model does not accurately describe the adsorption of malachite green to the gold nanoparticle surface. The modified Langmuir model has a much better fit to the experimental results, yielding $K = 2.1 \pm 1.4 \times 10^{11}$, $\Delta G° = -15.4 \pm 0.4$ kcal/mol, and $N_{max} = 125 \pm 4$ nM. Dividing N_{max} by the nanoparticle concentration determined from Figure 2 gives $1.13 \pm 0.04 \times 10^3$ sites per nanoparticle, where each site occupies 71 ± 14 A^2. The measured site area is consistent with the molecular footprint from a monolayer of MG oriented primarily perpendicular to the nanoparticle surface.

Additionally, these measurements indicate that malachite green binds more strongly and at a higher site density to gold nanoparticles than to either polystyrene microparticles or oil droplets in water at a similar pH. The free energy of adsorption of MG to 1.05 ± 0.03 µm polystyrene sulfate microspheres in water has been previously measured to be -11.1 ± 0.1 kcal/mol with a maximum of $1.8 \pm 0.2 \times 10^6$ sites per particle where each site occupies 192 ± 24 A^2 [30]. Similarly, the free energy of adsorption of MG to 230 ± 3 nm oil droplets in water has been previously measured to be -11.5 ± 0.4 kcal/mol with a maximum of $1.2 \pm 0.1 \times 10^5$ sites per particle where each site occupies 145 ± 10 A^2 [30]. The free energy of adsorption of MG is approximately 4 kcal/mol more attractive to the gold nanoparticle surface than to the colloidal polystyrene microparticles and to the oil droplets in water. The MG adsorbate site density on the gold nanoparticles is approximately three times greater than on polystyrene and approximately two times greater than on oil droplets in water. The origin of these differences in adsorption free energies and site densities for MG to gold nanoparticles relative to polystyrene and emulsion particle surfaces is not known at this time. An important factor that we are investigating is the charge densities of the particles themselves. A higher surface charge density of these negatively charged particles would increase the electrostatic contribution to the adsorption free energy of the positively charged MG molecule. What role the metal plays, e.g. image charge attraction of MG, is also being investigated.

4. Conclusions

Second harmonic generation has been used for the first time to probe freely adsorbing molecules that are located at the interface of metallic nanoparticles with the liquid in which they are suspended. The isotherm of malachite green adsorption to the surface of colloidal gold nanoparticles in aqueous solution has been obtained from measurements of the SHG signal as a function of the adsorbate bulk concentration. The experimental results compare favorably to a modified Langmuir model that includes the depletion of the MG molecules in the bulk solution due to their adsorption to the gold nanoparticles. The free energy of adsorption is determined to be -15.4 ± 0.4 kcal/mol. Additionally, it is determined that there are $1.13 \pm 0.04 \times 10^3$ adsorbate sites per nanoparticle with each site occupying 71 ± 14 A^2. Compared to SHG measurements of other colloidal particles, it is found that MG adsorbs more strongly and at a higher site density to gold nanopar-

ticles than to either polystyrene microparticles or oil droplets in water. The origin of these differences in terms of particle surface charge density due to the charged capping groups and also in terms of the interactions of the adsorbate molecules with the gold nanoparticle itself is being investigated.

Acknowledgements

References

[1] S. Link, M.A. El-Sayed, Int. Rev. Phys. Chem. 19 (2000) 409.
[2] M.-C. Daniel, D. Astruc, Chem. Rev. 104 (2004) 293.
[3] R.A. Sperling, P.R. Gil, F. Zhang, M. Zanella, W.J. Parak, Chem. Soc. Rev. 37 (2008) 1896.
[4] P.L. Stiles, J.A. Dieringer, N.C. Shah, R.P. Van Duyne, Annu. Rev. Anal. Chem. 1 (2008) 601.
[5] L. Brus, Acc. Chem. Res. 41 (2008) 1742.
[6] J.R. Lakowicz, Anal. Biochem. 337 (2005) 171.
[7] F. Tam, G.P. Goodrich, B.R. Johnson, N.J. Halas, Nano Lett. 7 (2007) 496.
[8] S. Baldelli, A.S. Eppler, E. Anderson, Y.-R. Shen, G.A. Somorjai, J. Chem. Phys. 113 (2000) 5432.
[9] A.N. Bordenyuk, C. Weeraman, A. Yatawara, H.D. Jayathilake, I. Stiopkin, Y. Liu, A.V. Benderskii, J. Phys. Chem. C 111 (2007) 8925.
[10] F.W. Vance, B.I. Lemon, J.T. Hupp, J. Phys. Chem. B 102 (1998) 10091.
[11] E.C. Hao, G.C. Schatz, R.C. Johnson, J.T. Hupp, J. Chem. Phys. 117 (2002) 5963.
[12] J.-P. Abid, J. Nappa, H.H. Girault, P.-F. Brevet, J. Chem. Phys. 121 (2004) 12577.
[13] J. Nappa, I. Russier-Antoine, E. Benichou, C. Jonin, P.F. Brevet, J. Chem. Phys. 125 (2006) 184712.
[14] S. Freddi et al., J. Phys. Chem. C 113 (2009) 2722.
[15] A.E. Prigodich, O.-S. Lee, W.L. Daniel, D.S. Seferos, G.C. Schatz, C.A. Mirkin, J. Am. Chem. Soc. 132 (2010) 10638.
[16] A. Saha, S.K. Basiruddin, R. Sarkar, N. Pradhan, N.R. Jana, J. Phys. Chem. C 113 (2009) 18492.
[17] X. Huang, I.H. El-Sayed, W. Qian, M.A. El-Sayed, J. Am. Chem. Soc. 128 (2006) 2115.
[18] K.B. Eisenthal, Chem. Rev. 106 (2006) 1462.
[19] J.I. Dadap, H.B. de Aguiar, S. Roke, J. Chem. Phys. 130 (2009) 214710.
[20] S. Roke, ChemPhysChem 10 (2009) 1380.
[21] A.G.F. de Beer, H.B. de Aguiar, J.F.W. Nijsen, S. Roke, Phys. Rev. Lett. 102 (2009) 095502.
[22] H.B. de Aguiar, A.G.F. de Beer, M.L. Strader, S. Roke, J. Am. Chem. Soc. 132 (2010) 2122.
[23] Y.R. Shen, The Principles of Nonlinear Optics, Wiley, Hoboken, 2003.
[24] J.I. Dadap, J. Shan, K.B. Eisenthal, T.F. Heinz, Phys. Rev. Lett. 83 (1999) 4045.
[25] N. Yang, W.E. Angerer, A.G. Yodh, Phys. Rev. Lett. 87 (2001) 103902.
[26] A.G.F. de Beer, S. Roke, Phys. Rev. B 79 (2009) 155420.
[27] E. Dulkeith et al., Phys. Rev. Lett. 89 (2002) 203002.
[28] T. Soller et al., Nano Lett. 7 (2007) 1941.
[29] H. Wang, E.C.Y. Yan, E. Borguet, K.B. Eisenthal, Chem. Phys. Lett. 259 (1996) 15.
[30] H. Wang, E.C.Y. Yan, Y. Liu, K.B. Eisenthal, J. Phys. Chem. B 102 (1998) 4446.
[31] H. Wang, T. Troxler, A.-G. Yeh, H.-L. Dai, Langmuir 16 (2000) 2475.
[32] H.M. Eckenrode, H.-L. Dai, Langmuir 20 (2004) 9202.
[33] H.M. Eckenrode, S.-H. Jen, J. Han, A.-G. Yeh, H.-L. Dai, J. Phys. Chem. B 109 (2005) 4646.
[34] S.-H. Jen, G. Gonella, H.-L. Dai, J. Phys. Chem. A 113 (2009) 4758.
[35] B. Schürer, W. Peukert, Particulate Sci. Tech. 28 (2010) 458.
[36] E.C.Y. Yan, K.B. Eisenthal, J. Phys. Chem. B 103 (1999) 6056.
[37] Y. Liu, J.I. Dadap, D. Zimdars, K.B. Eisenthal, J. Phys. Chem. B 103 (1999) 2480.
[38] H. Wang, T. Troxler, A.-G. Yeh, H.-L. Dai, J. Phys. Chem. C 111 (2007) 8708.
[39] A. Srivastava, K.B. Eisenthal, Chem. Phys. Lett. 292 (1998) 345.
[40] J. Liu, M. Subir, K. Nguyen, K.B. Eisenthal, J. Phys. Chem. B 112 (2008) 15263.
[41] E.C.Y. Yan, Y. Liu, K.B. Eisenthal, J. Phys. Chem. B 102 (1998) 6331.
[42] M. Subir, J. Liu, K.B. Eisenthal, J. Phys. Chem. C 112 (2008) 15809.
[43] X. Ji, X. Song, J. Li, Y. Bai, W. Yang, X. Peng, J. Am. Chem. Soc. 129 (2007) 13939.
[44] C.F. Bohren, D.R. Huffman, Absorption and Scattering of Light by Small Particles, Wiley, New York, 1998.
[45] A.C. Bhasikuttan, A.V. Sapre, T. Okada, J. Phys. Chem. A 107 (2003) 3030.